BUTTERWORTH HEINEMANN

Polymer Vol. 36 No. 1, pp. 155–167, 1995

0032-3861/95/$10.00+0.00

Effects of sample preparation and flow geometry on the rheological behaviour and morphology of microphase-separated block copolymers: comparison of cone-and-plate and capillary data

James H. Han and Daan Feng
Research and Development, Amoco Chemical Company, Naperville, IL 60566, USA

and Chin Choi-Feng
Research and Development, Amoco Corporation, Naperville, IL 60566, USA

and Chang Dae Han*
Department of Polymer Engineering, The University of Akron, Akron, OH 44325, USA
(Received 14 May 1993; revised 19 May 1994)

The steady shear viscosities of two microphase-separated triblock copolymers, a polystyrene-*block*-polybutadiene-*block*-polystyrene copolymer (Kraton 1102) and a polystyrene-*block*-polyisoprene-*block*-polystyrene copolymer (Kraton 1107), were measured at various temperatures, using a cone-and-plate rheometer at low shear rates (ca. 0.01–10 s^{-1}) and a capillary rheometer at high shear rates (ca. 5–5000 s^{-1}). In order to investigate the effect of sample preparation on the viscosity, specimens of Kraton 1102 were prepared using two different methods: (a) solvent film casting and (b) compression moulding. Samples of Kraton 1107 were prepared only by compression moulding. In the present study we found that (a) for compression-moulded specimens the shear viscosities obtained using a cone-and-plate rheometer did *not* overlap those obtained using a capillary rheometer, while for solvent-cast specimens there was a reasonably good agreement between the two, and (b) the viscosities of solvent-cast specimens were much lower than those of compression-moulded specimens. This observation was explained with the aid of transmission electron micrographs, which were taken of ultrathin sections cut parallel and perpendicular to the direction of shear. We found from transmission electron micrographs that the application of steady shear flow affected greatly the morphology of Kraton 1102 having cylindrical microdomains of polystyrene phase, whereas it affected little the morphology of Kraton 1107 having spherical microdomains of polystyrene phase. Also measured were the complex shear viscosities of the two block copolymers at various temperatures. We have shown that neither time–temperature superposition nor the Cox–Merz rule is applicable to microphase-separated block copolymers.

(Keywords: block copolymer; microdomains; steady shear viscosity)

INTRODUCTION

A better understanding of the rheological behaviour of complex polymer systems, such as two-phase polymer mixtures, microphase-separated block copolymers and liquid-crystalline polymers, is of fundamental and technological importance. It has been shown that the rheological behaviour of, for instance, two-phase polymer mixtures depends strongly upon the morphological state that exists under the particular flow conditions concerned[1]. This subject was brought to light in the 1970s by a series of papers of Han and coworkers[2–7], who investigated the rheological behaviour of blends of two incompatible polymers. Although the morphology of block copolymers is quite different from that of two-phase polymer blends, the importance of relating the rheological properties with morphology in block copolymers should also be emphasized.

In the past, a number of research groups[8–22] reported on the rheological properties of block copolymers: some investigators[8–12] reported on the steady shear flow properties and others[10,12,13–22] reported on the oscillatory shear flow properties. Only a few research groups[9,12] compared the steady shear flow properties of block copolymers determined from a cone-and-plate rheometer with those determined from a capillary rheometer, and showed that these two sets of data did not always overlap each other at the same shear rate. However, to the best

*To whom correspondence should be addressed

of our knowledge, to date no attempt, on the basis of scientific evidence (e.g. micrographs of samples), has been reported to explain such experimental observations.

It is well documented in the literature[19-21] that the rheological behaviour of a block copolymer depends on both molecular weight and block copolymer composition (or block length ratio), and that steady shear viscosity or complex shear viscosity exhibits Newtonian behaviour when the block copolymer is heated to a temperature above a certain critical value (often referred to as the order–disorder transition temperature, T_{ODT}), at which all the microdomains in the block copolymer are solubilized, forming a homogeneous phase. Note that block length ratio controls microdomain structure (spheres, cylinders, lamellae or ordered bicontinuous double diamonds)[23-28]. Han and coworkers[19-21] have suggested a rheological criterion that enables one to determine the T_{ODT} of a block copolymer.

Recently, we investigated the rheological behaviour of microphase-separated ABA-type triblock copolymers, with emphasis on the effects of the type of rheometer and the method of sample preparation employed. In order to explain the differences in the rheological behaviour observed with different types of rheometers or with different methods of sample preparation, we utilized transmission electron microscopy to examine ultrathin sections of the specimens collected before and after the shear flow experiments. In this paper we shall report the highlights of our findings.

EXPERIMENTAL

Materials

In this study we used two commercial ABA-type triblock copolymers, Kraton 1102 and Kraton 1107, both supplied by Shell Development Company. Note that Kraton 1102 is a polystyrene-*block*-polybutadiene-*block*-polystyrene (SBS) copolymer and Kraton 1107 is a polystyrene-*block*-polyisoprene-*block*-polystyrene (SIS) copolymer. Kraton 1102 has the SBS block molecular weights 10430–53600–10430, and Kraton 1107 has the SIS block molecular weights 10000–120000–10000.

Sample preparation

It has been reported in the literature[24,25] that the microdomain structure of a block copolymer varies with the method of sample preparation. Under such circumstances, the rheological properties may also be affected by the method of sample preparation, because the rheological properties are, in general, dependent upon the morphology of the samples. Therefore, in order to investigate the effect of the method of sample preparation on the rheological properties of the block copolymers, in the present study samples of Kraton 1102 were prepared using both compression moulding and solvent casting. Samples of Kraton 1107 were prepared using only compression moulding. Compression-moulded samples were prepared at 180°C.

When preparing samples by solvent casting, Kraton 1102 was dissolved in toluene (10% solid in solution) in the presence of an antioxidant (0.1 wt% Irganox 1010, Ciba-Geigy Co.) and then the solvent was evaporated very slowly. The evaporation of solvent was carried out initially in a fume hood at room temperature for a week and then in a vacuum oven at 40°C for three days. The last trace of solvent was removed by drying the sample in a vacuum oven at elevated temperature by gradually raising the oven temperature up to 110°C. Drying of the sample was continued until there was no further change in weight. Finally, the sample was annealed at 130°C for 10 h. The solvent-cast sheet was cut into small pieces, so that they could be loaded into the barrel of the capillary rheometer. For the cone-and-plate rheometer, the solvent-cast sheet was cut into a small disc having the diameter of about 25 mm, which was then placed in the cone-and-plate fixture.

Rheological measurement

A Rheometrics Dynamic Analyzer (model RDA-II) in the cone-and-plate (25 mm diameter plate and 0.1 radian cone angle) configuration was used to measure, in the steady shear mode, shear viscosity (η) as a function of shear rate ($\dot{\gamma}$) ranging from 0.01 to 10 s^{-1}, and, in the oscillatory shear mode, dynamic storage modulus (G') and dynamic loss modulus (G'') as a function of angular frequency (ω) ranging from 0.01 to 500 rad s^{-1}. The absolute value of complex viscosity was calculated using $|\eta^*(\omega)| = \{[G'(\omega)/\omega]^2 + [G''(\omega)/\omega]^2\}^{1/2}$. According to a previous study by Han and coworkers[20], the T_{ODT} of Kraton 1102 is 220°C and the T_{ODT} of Kraton 1107 is 230°C. Hence, in the present study rheological measurements were taken at temperatures below the T_{ODT} values of the respective block copolymers, i.e. in the ordered (or microphase-separated) state. All experiments were conducted in the presence of nitrogen in order to preclude oxidative degradation of the specimen.

Also employed was a capillary rheometer, Goettfert High Pressure Rheometer (Rheograph 2002), with four different capillary dies: (1) 1 mm diameter and 20 mm long, (2) 1 mm diameter and 30 mm long, (3) 0.5 mm diameter and 20 mm long, and (4) 0.5 mm diameter and 30 mm long. The capillary rheometer enabled us to obtain shear viscosities at high shear rates, not obtainable with the cone-and-plate rheometer. In the analysis of the capillary data, we neglected end corrections to calculate

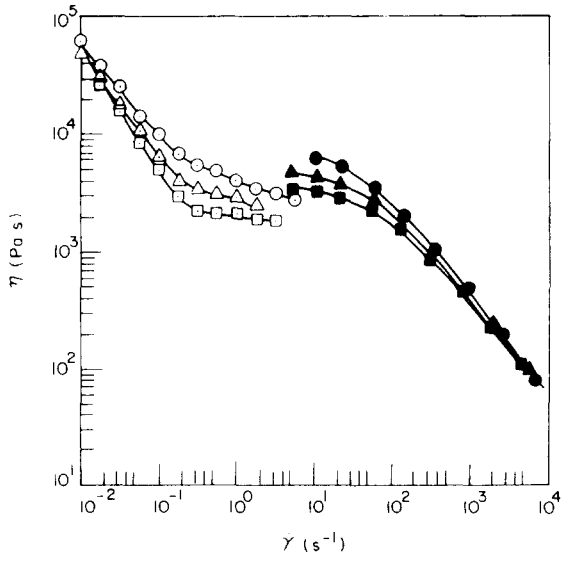

Figure 1 Plots of log $\dot{\gamma}$ for compression-moulded Kraton 1102 specimens at (○, ●) 160°C, (△, ▲) 170°C and (□, ■) 180°C. Open symbols are cone-and-plate data and filled symbols are capillary data

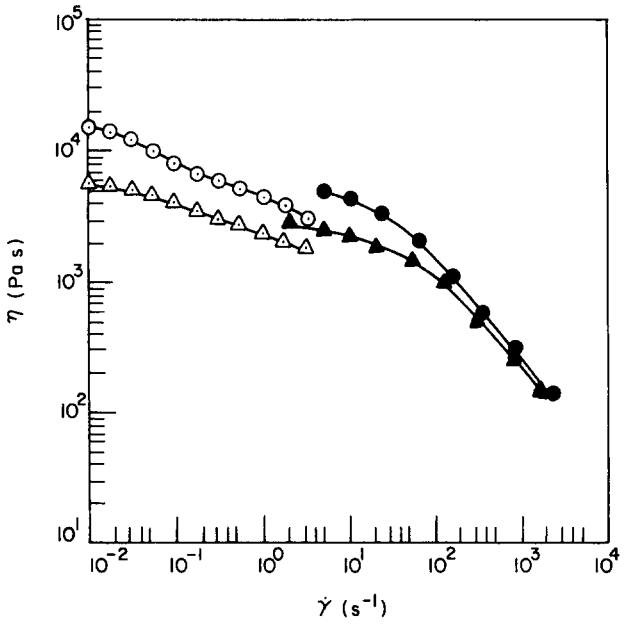

Figure 2 Plots of log η *versus* log $\dot{\gamma}$ for compression-moulded Kraton 1107 specimens at (⊙, ●) 180°C and (△, ▲) 200°C. Open symbols are cone-and-plate data and filled symbols are capillary data

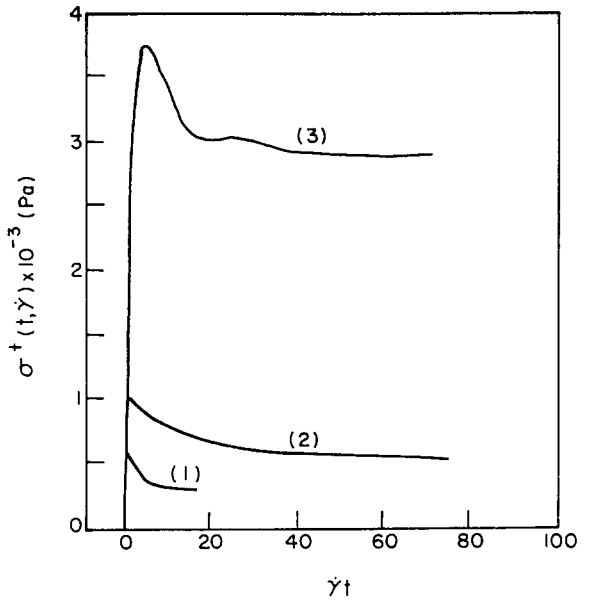

Figure 3 Traces of $\sigma^+(t, \dot{\gamma})$ *versus* $\dot{\gamma}t$ for solvent-cast Kraton 1102 specimens at 180°C, by varying $\dot{\gamma}$ stepwise: curve 1 at $\dot{\gamma}=0.01\ s^{-1}$; curve 2 at $\dot{\gamma}=0.1\ s^{-1}$; curve 3 at $\dot{\gamma}=1\ s^{-1}$

the viscosity. In presenting below the results of steady shear viscosities obtained from the capillary rheometer, we calculated *true* shear rates using the Rabinowitch–Mooney correction, and thus we shall present true shear viscosities to compare with the values of viscosities obtained from the cone-and-plate rheometer.

Transmission electron microscopy (TEM)

A transmission electron microscope (Philips 400T) was used to examine the microstructure of the block copolymer specimens before and/or after the shear flow experiment. Ultrathin sections of the specimens were obtained by microtoming at −90°C with a Reichert–Jung Cryoultramicrotome, and the rubbery component (polybutadiene in Kraton 1102 or polyisoprene in Kraton 1107) was selectively stained by exposure to osmium tetroxide vapour for 90 min, giving rise to dark areas in the micrographs taken.

RESULTS

Steady shear viscosity of microphase-separated block copolymers

Compression-moulded specimens. Figure 1 gives plots of log η *versus* log $\dot{\gamma}$ for compression-moulded Kraton 1102 specimens at 160, 170 and 180°C, and *Figure 2* gives plots of log η *versus* log $\dot{\gamma}$ for compression-moulded Kraton 1107 specimens at 180 and 200°C, where open symbols represent cone-and-plate data and filled symbols represent capillary data. It can be seen in *Figures 1* and *2* that, within experimental uncertainties, the viscosities measured using a cone-and-plate rheometer do not overlap those measured using a capillary rheometer.

In obtaining the data presented in *Figures 1* and *2*, we made certain that steady state was achieved in each experimental run. To illustrate the point, *Figure 3* gives plots of shear stress growth $\sigma^+(t, \dot{\gamma})$, upon start-up of shear flow in the cone-and-plate rheometer, *versus* shear

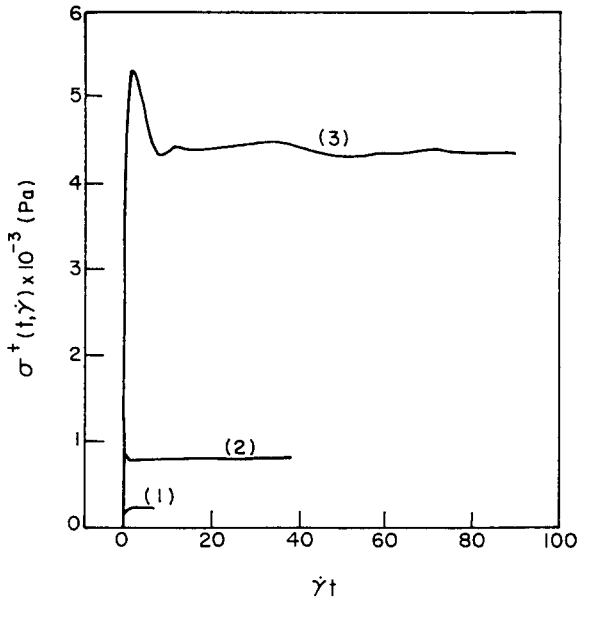

Figure 4 Traces of $\sigma^+(t, \dot{\gamma})$ *versus* $\dot{\gamma}t$ for compression-moulded Kraton 1107 specimens at 180°C, by varying $\dot{\gamma}$ stepwise: curve 1 at $\dot{\gamma}=0.01\ s^{-1}$; curve 2 at $\dot{\gamma}=0.1\ s^{-1}$; curve 3 at $\dot{\gamma}=1\ s^{-1}$

strain ($\dot{\gamma}t$) for Kraton 1102 at 180°C for $\dot{\gamma}$ at 0.01, 0.1 and 1.0 s^{-1}, respectively. Similar plots are given in *Figure 4* for Kraton 1107 at 180°C for $\dot{\gamma}$ at 0.01, 0.1 and 1.0 s^{-1}, respectively, Note in *Figures 3* and *4* that t denotes the time during which the specimen was sheared. Thus, in the use of the cone-and-plate rheometer, we calculated values of η at each given $\dot{\gamma}$ only after the shear stress levelled off to an equilibrium value.

In the use of the capillary rheometer, we increased the length-to-diameter ratio (L/D) from 20 to 60 in order to determine the value of L/D that is sufficiently high to enable us to neglect, for all intents and purposes, the

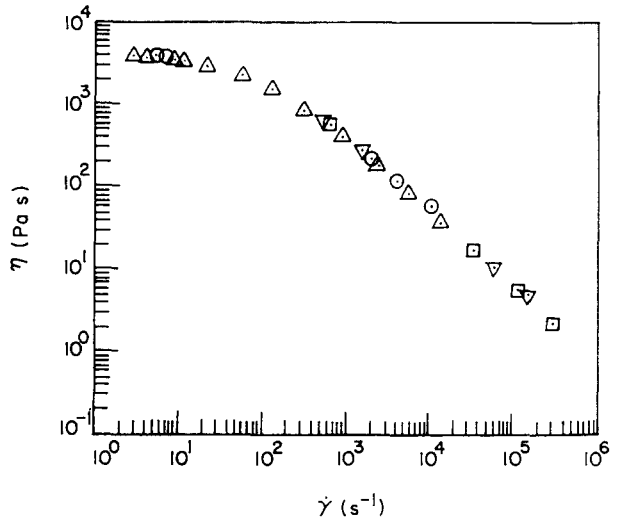

Figure 5 Plots of log η *versus* log $\dot{\gamma}$ for compression-moulded Kraton 1102 specimens at 180°C, obtained with the capillary rheometer having length-to-diameter ratios (L/D): (⊙) 20; (△) 30; (⊡) 40; (▽) 60

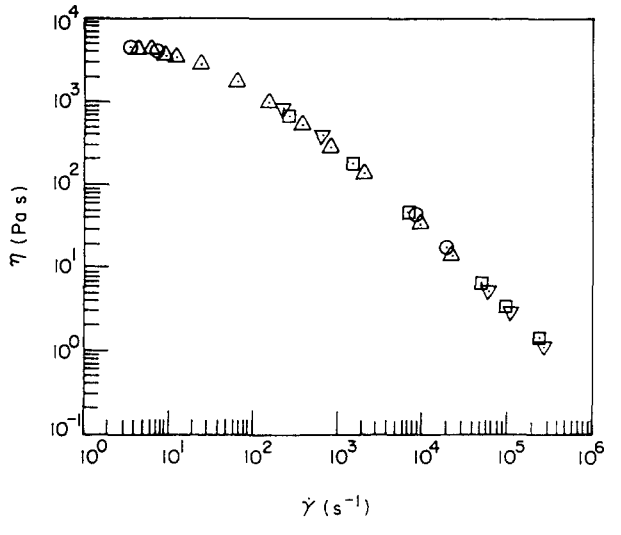

Figure 6 Plots of log η *versus* log $\dot{\gamma}$ for compression-moulded Kraton 1107 specimens at 180°C, obtained with the capillary rheometer having length-to-diameter ratios (L/D): (⊙) 20; (△) 30; (⊡) 40; (▽) 60

end corrections. *Figure 5* gives plots of log η *versus* log $\dot{\gamma}$ for Kraton 1102 at 180°C, which were obtained using four different values of L/D, 20, 30, 40 and 60. Similar plots for Kraton 1107 at 180°C are given in *Figure 6*, which were also obtained using four different values of L/D, 20, 30, 40 and 60. Note that the values of η given in *Figures 5* and *6* were calculated by neglecting the end corrections. It can be seen in *Figures 5* and *6* that the four different values of L/D employed give rise to essentially identical results, leading us to conclude that $L/D \geqslant 20$ is sufficiently large for us to be able to neglect the end corrections.

It is appropriate to mention at this juncture that in the past other research groups also compared the rheological properties of block copolymers measured using different types of rheometers. The results reported in the literature are very confusing. In 1969, using Kraton 1102 and three other grades of SBS triblock copolymers having almost the same weight fraction (0.266–0.274) of polystyrene but different total molecular weights, Holden *et al.*[9] reported that the viscosities measured using a cone-and-plate rheometer agreed well with those measured using a capillary rheometer (see figure 4 of ref. 9). However, for an SBS block copolymer having the SBS block molecular weights of 16 000–52 000–16 000 and the weight fraction of 0.39 for polystyrene (see figure 6 of ref. 9), the same authors reported that the viscosities measured using a capillary rheometer did not agree with those measured with a cone-and-plate rheometer; specifically, the viscosity measured using a capillary rheometer at a shear rate of about 1 s^{-1} was almost an order of magnitude greater than that measured using a cone-and-plate rheometer. Holden *et al.* did not offer any explanation as to why the two sets of block copolymers exhibited different rheological responses when using either a cone-and-plate rheometer or a capillary rheometer.

About a decade later, in 1980 Ghijsels and Raadsen[12] reported the steady shear viscosities of an SBS block copolymer (Cariflex TR 1200, Shell Chemical Company) having the SBS block molecular weights of 11 000–56 000–11 000, which is very close to Kraton 1102. The study reported by Ghijsels and Raadsen was the outcome of a joint research effort at several research laboratories in different parts of the world, which was organized by the IUPAC Working Party on 'Structure and Properties of Commercial Polymers'. *Figure 7* gives, for comparison, plots of log η *versus* log $\dot{\gamma}$ for Cariflex TR 1200 at 150°C, which was prepared using Figures 2 and 10 in ref. 12. It can be seen in *Figure 7* that the values of η of Cariflex TR 1200 measured by different research groups using capillary rheometers agree rather well, but the data obtained by the same research groups using cone-and-plate rheometers show considerable scatter. In other words, the η data obtained by one research group (symbol ◇) give a reasonably good overlap between the cone-and-plate and capillary data, while the data obtained by other research groups (symbols ⊙, ⊡, ▽) do not. We cannot explain the source(s) of the disagreement observed in *Figure 7*. Note that the data

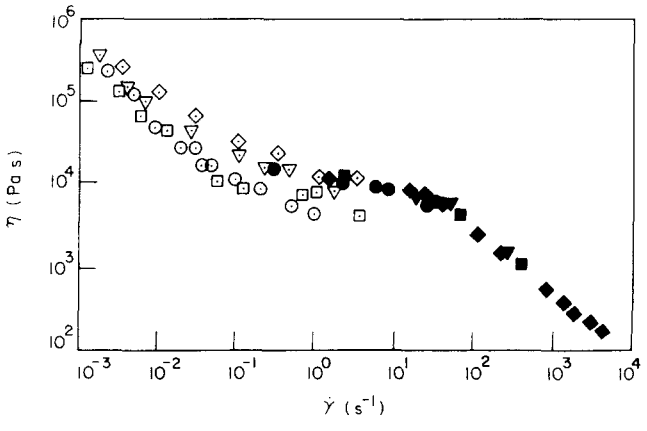

Figure 7 Plots of log η *versus* log $\dot{\gamma}$ for Cariflex TR 1200 at 150°C. The plots were prepared from figures 2 and 10 in ref. 12. Note that the measurements were taken by various research laboratories: (⊙, ●) BASF in Germany; (⊡, ■) Institute of Petrochemical Synthesis in USSR; (◇, ◆) Montedison in Italy; (▽, ▼) Shell Amsterdam in The Netherlands. Open symbols are cone-and-plate data and filled symbols are capillary data

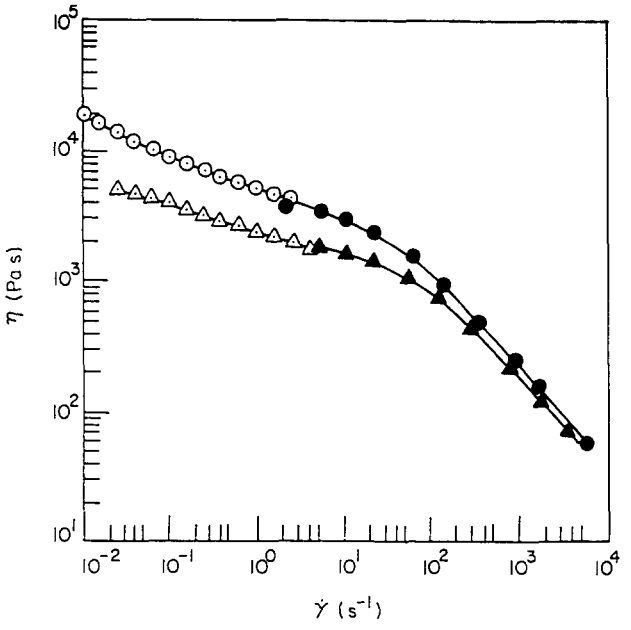

Figure 8 Plots of $\log \eta$ *versus* $\log \dot{\gamma}$ for solvent-cast Kraton 1102 specimens at (⊙, ●) 180°C and (△, ▲) 200°C. Open symbols are cone-and-plate data and filled symbols are capillary data

given in *Figure 7* were taken using either compression-moulded specimens or crumbs as received from the manufacturer.

However, we are of the opinion that there is no reason why the rheological properties of morphologically complex polymer systems, such as the block copolymers under consideration here, should show agreement between cone-and-plate and capillary measurements, because the morphological state of a block copolymer in a cone-and-plate rheometer can be different from that in a capillary rheometer. In other words, the morphology of a block copolymer may depend on the intensity of the shear flow field to which the block copolymer is subjected. Below we shall further elaborate on this by presenting transmission electron micrographs taken of the specimens that were sheared either in a cone-and-plate rheometer or in a capillary rheometer.

Solvent-cast specimens. Figure 8 gives plots of $\log \eta$ *versus* $\log \dot{\gamma}$ for solvent-cast Kraton 1102 specimens at 180 and 200°C. It can be seen in *Figure 8* that the values of η measured using a cone-and-plate rheometer overlap reasonably well with those measured using a capillary rheometer. This is at variance with the observation made for the compression-moulded Kraton 1102 specimens (see *Figure 1*). The comparison of *Figure 8* (symbol ⊙) with *Figure 1* (symbol ⊡) at 180°C reveals further that (a) at low $\dot{\gamma}$ (i.e. in the cone-and-plate rheometer) shear-thinning behaviour is much more intense for the compression-moulded specimens than for solvent-cast specimens, and (b) at high $\dot{\gamma}$ (i.e. in the capillary rheometer) the values of η are higher for the compression-moulded specimens than for the solvent-cast specimens. We found that the compression-moulded specimens were thermally much more unstable than the solvent-cast specimens. This is the reason why the range of measurement temperatures employed for compression-moulded specimens was lower than that for solvent-cast specimens. It should be mentioned that, as described in the 'Experimental' section, an antioxidant (Irganox 1010) was added during the preparation of samples by solvent casting. Below we shall elaborate on the thermal stability of the block copolymers employed in this study.

We conclude from *Figures 1* and *8* that different methods of sample preparation appear to give rise to different rheological responses in both cone-and-plate and capillary rheometers. When presenting below transmission electron micrographs of the specimens that had been sheared in a cone-and-plate or capillary rheometer, we shall offer an explanation as to why the shear-dependent behaviour of viscosity observed in this study is so different between compression-moulded specimens and solvent-cast specimens.

Complex shear viscosity of microphase-separated block copolymers

Figure 9 gives plots of $\log|\eta^*|$ *versus* $\log \omega$ (symbol ◑) for compression-moulded Kraton 1102 specimens at 160°C. Also given in *Figure 9*, for comparison, are plots of $\log \eta$ *versus* $\log \dot{\gamma}$ obtained from a cone-and-plate rheometer (symbol ⊙) and from a capillary rheometer (symbol ●). It can be seen in *Figure 9* that the values of η obtained from the cone-and-plate rheometer are much lower than those of $|\eta^*|$, whereas the values of η obtained from the capillary rheometer are higher than those of $|\eta^*|$. In 1980 Ghijsels and Raadsen[12] also reported that for compression-moulded Cariflex TR 1200, which is very similar to Kraton 1102 used in the present study, η was found to be considerably lower than $|\eta^*|$ at $\dot{\gamma}=\omega$ for $\dot{\gamma}<1\ s^{-1}$.

Further observations are worth noting in *Figure 9*. (1) Even at very low $\dot{\gamma}$ (0.01–1 s^{-1}) in steady shear flow, the η decreased initially very rapidly with increasing $\dot{\gamma}$ and then showed a plateau region as the $\dot{\gamma}$ was increased further. (2) On the other hand, in oscillatory shear flow, $|\eta^*|$ decreased steadily with increasing ω. In view of the

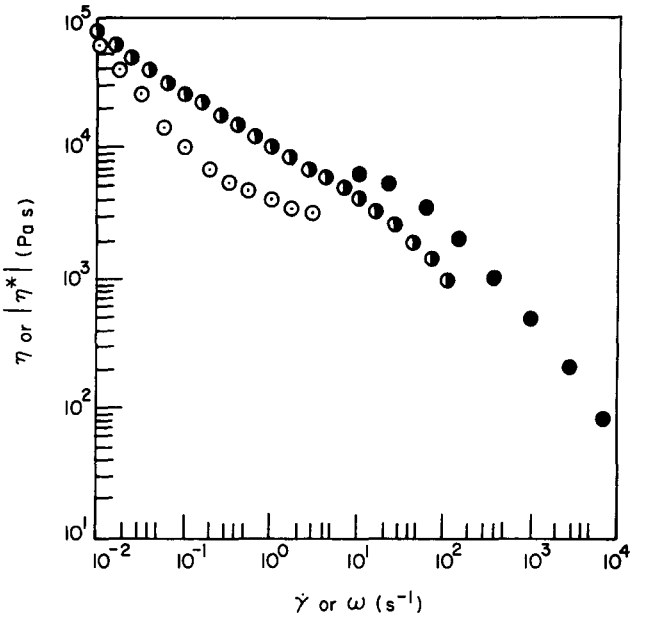

Figure 9 Comparison of $|\eta^*|$ with η for compression-moulded K1102 specimens at 160°C: (◑) plot of $\log|\eta^*|$ *versus* $\log \omega$; (⊙) plot of $\log \eta$ *versus* $\log \dot{\gamma}$ from a cone-and-plate rheometer; (●) plot of $\log \eta$ *versus* $\log \dot{\gamma}$ from a capillary rheometer

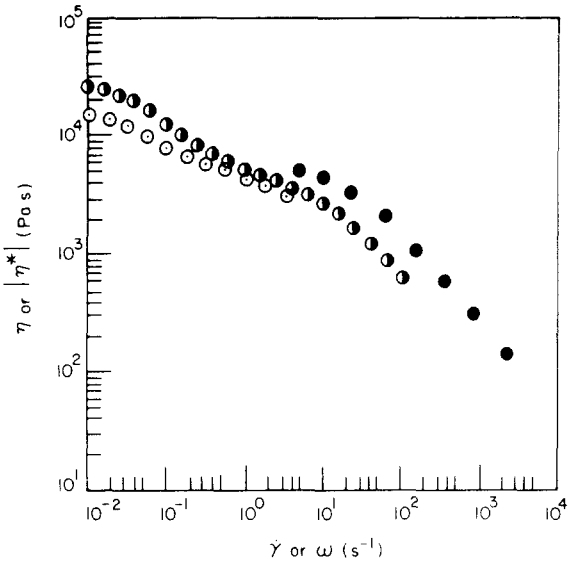

Figure 10 Comparison of $|\eta^*|$ with η for compression-moulded K1107 specimens at 180°C: (◑) plot of $\log|\eta^*|$ *versus* $\log\omega$; (⊙) plot of $\log\eta$ *versus* $\log\dot{\gamma}$ from a cone-and-plate rheometer; (●) plot of $\log\eta$ *versus* $\log\dot{\gamma}$ from a capillary rheometer

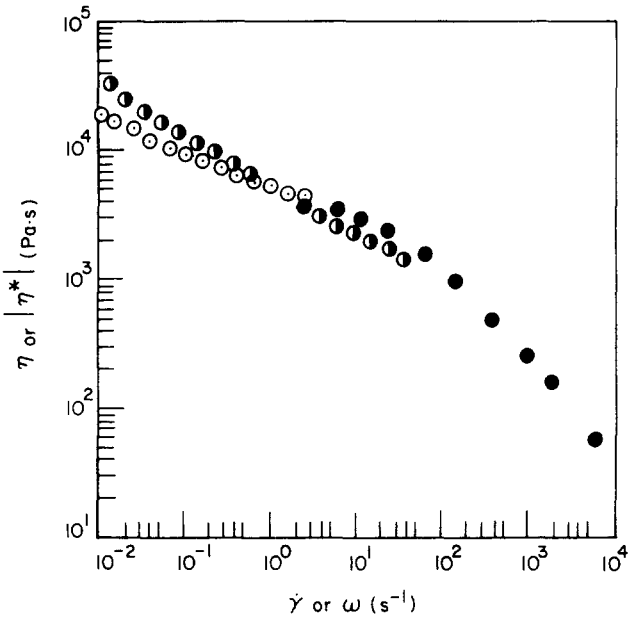

Figure 11 Comparison of $|\eta^*|$ with η for solvent-cast K1102 specimens at 180°C: (◑) plot of $\log|\eta^*|$ *versus* $\log\omega$; (⊙) plot of $\log\eta$ *versus* $\log\dot{\gamma}$ from a cone-and-plate rheometer; (●) plot of $\log\eta$ *versus* $\log\dot{\gamma}$ from a capillary rheometer

fact that Kraton 1102 has cylindrical microdomains[19] (also will be shown below), the rapid decrease in η with increasing $\dot{\gamma}$ observed in *Figure 9* may be attributable to variations in the morphological state of the specimen taking place during shear flow. Below we shall present evidence showing that indeed such speculation is correct.

Figure 10 compares $|\eta^*|$ with η for compression-moulded Kraton 1107 specimens at 180°C. It can be seen in *Figure 10* that, at low $\dot{\gamma}$ (0.01–1 s^{-1}), the differences between $|\eta^*|$ and η for compression-moulded Kraton 1107 specimens are not as large as those for compression-moulded Kraton 1102 specimens (see *Figure 9*), although the values of η are still lower than those of $|\eta^*|$, and that the values of η at high $\dot{\gamma}$ obtained by the capillary rheometer are much higher than those of $|\eta^*|$. The relatively small differences between $|\eta^*|$ and η for compression-moulded Kraton 1107 specimens, observed in *Figure 10*, seem to suggest that the morphological state of the specimens might not have changed much during shear flow. Below we shall present evidence supporting such an interpretation. Note that Kraton 1107 has spherical microdomains.

Figure 11 compares $|\eta^*|$ with η for solvent-cast Kraton 1102 specimens at 180°C. It can be seen in *Figure 11* that the plot of $\log|\eta^*|$ *versus* $\log\omega$ crosses the plot of $\log\eta$ *versus* $\log\dot{\gamma}$. A comparison of *Figure 11* and *Figure 9* reveals that the differences between $|\eta^*|$ and η for the solvent-cast specimens are much smaller than those for the compression-moulded specimens, suggesting that the morphological state of the solvent-cast Kraton 1102 specimens might not have changed much during shear flow. This speculation will be proven to be valid when presenting below transmission electron micrographs. On the basis of *Figures 9–11* we can conclude that the Cox–Merz rule[29] does not hold for Kraton 1102 and Kraton 1107 and hence for microphase-separated block copolymers in general.

Phase morphology of microphase-separated block copolymers as affected by shear flow

Below we shall first present the differences in morphology, as examined by TEM, between compression-moulded and solvent-cast specimens of Kraton 1102, and then see how much, if at all, the morphology of the block copolymer was affected by shear flow in cone-and-plate and capillary rheometers, respectively. It should be mentioned that in the present study the sheared specimens were collected, upon completion of rheological measurement, by quenching very rapidly with the aid of liquid nitrogen.

Figure 12 gives transmission electron micrographs taken at room temperature of ultrathin sections of as-received Kraton 1102 specimens: (a) before being subjected to steady shear flow; (b) cut, after being sheared at $\dot{\gamma} = 10\ s^{-1}$ in a cone-and-plate rheometer at 200°C, parallel to the shear direction; (c) cut, after being sheared at $\dot{\gamma} = 100\ s^{-1}$ in a capillary rheometer at 200°C, parallel to the extrusion direction; and (d) cut, after being sheared at $\dot{\gamma} = 100\ s^{-1}$ in a capillary rheometer at 200°C, perpendicular to the extrusion direction. The following observations are worth noting in *Figure 12*. (1) In *Figure 12a* we observe that the polystyrene (PS) microdomains (white areas) with the average size of ca. 20 nm are distributed more or less randomly in the rubbery polybutadiene (PB) matrix (dark areas); in other words, the as-received Kraton 1102 does not show any regular morphology, and the PS microdomains have different sizes and shapes. (2) However, as may be seen in *Figure 12b*, when subjected to steady shear flow in a cone-and-plate rheometer at $\dot{\gamma} = 10\ s^{-1}$, the compression-moulded Kraton 1102 specimen has a morphology consisting of long rods of PS phase aligned parallel to the direction of shear. (3) It is of interest to observe in *Figure 12c* that, when a compression-moulded Kraton 1102 specimen was subjected to steady shear flow at $\dot{\gamma} = 100\ s^{-1}$ in a capillary die having an L/D ratio of 30, its morphology consists of long rods, somewhat

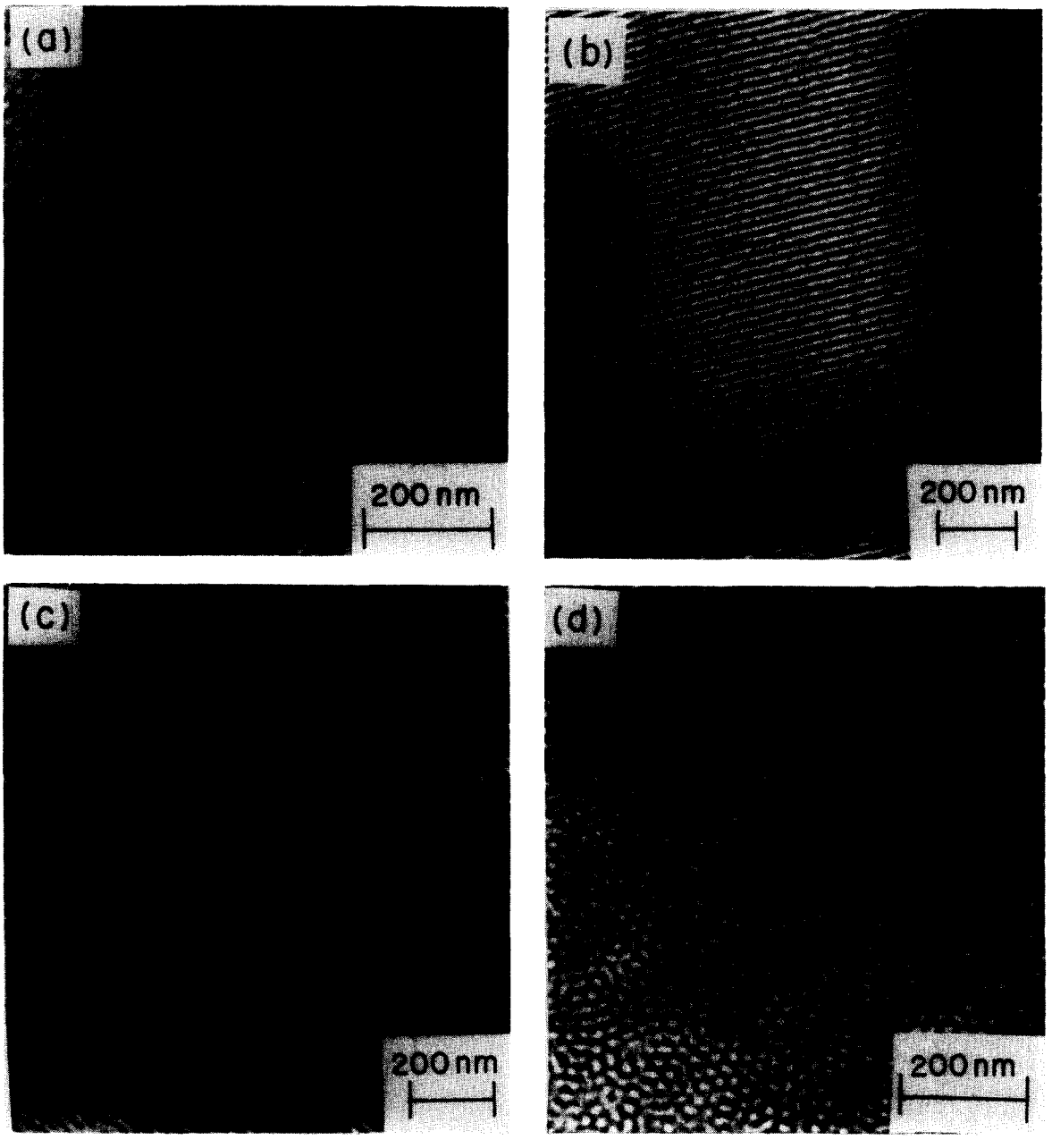

Figure 12 Transmission electron micrographs of ultrathin sections of compression-moulded Kraton 1102 specimens: (a) before being subjected to steady shear flow; (b) cut, after being subjected to steady shear flow at $\dot{\gamma} = 10\ s^{-1}$ in a cone-and-plate rheometer at 200°C, parallel to the shear direction; (c) cut, after being subjected to steady shear flow at $\dot{\gamma} = 100\ s^{-1}$ in a capillary rheometer at 200°C, parallel to the direction of extrusion; (d) cut, after being subjected to steady shear flow at $\dot{\gamma} = 100\ s^{-1}$ in a capillary rheometer at 200°C, perpendicular to the direction of extrusion

non-uniform (irregular) in diameter, of the PS phase aligned along the direction of extrusion. The claim that the PS microdomains in *Figure 12c* are cylinders is supported by the micrograph of the cross-section of the extrudate, given in *Figure 12d*, showing more or less a round shape of the PS phase (white area) dispersed in the rubbery matrix (dark area). It should be mentioned that previously Keller and coworkers[30,31] and Pedemonte and coworkers[32] reported the morphology of SBS triblock copolymers having about 30 wt% PS block, exhibiting continuous rods of PS phase in the PB matrix, when extruded in a capillary die. The seemingly unstable rods of the PS phase in *Figure 12c* appear to suggest that break-up of long rods of PS phase was about to take place inside the capillary.

The dramatic change in the morphological state of the compression-moulded Kraton 1102 specimen (compare *Figure 12a* with *Figure 12b*), when sheared at $\dot{\gamma} = 10\ s^{-1}$ in a cone-and-plate rheometer, now seems to explain why such a rapid drop in η occurred as $\dot{\gamma}$ was increased from 0.01 to $1\ s^{-1}$ (see *Figure 1*).

Figure 13 gives transmission electron micrographs taken at room temperature of ultrathin sections of compression-moulded Kraton 1107 specimens: (a) before being subjected to steady shear flow; (b) cut, after being sheared at $\dot{\gamma} = 10\ s^{-1}$ in a cone-and-plate rheometer at 200°C, parallel to the direction of shear flow; (c) cut, after being sheared at $\dot{\gamma} = 100\ s^{-1}$ in a capillary rheometer at 200°C, parallel to the direction of extrusion; and (d) cut, after being sheared at $\dot{\gamma} = 100\ s^{-1}$ in a capillary rheometer

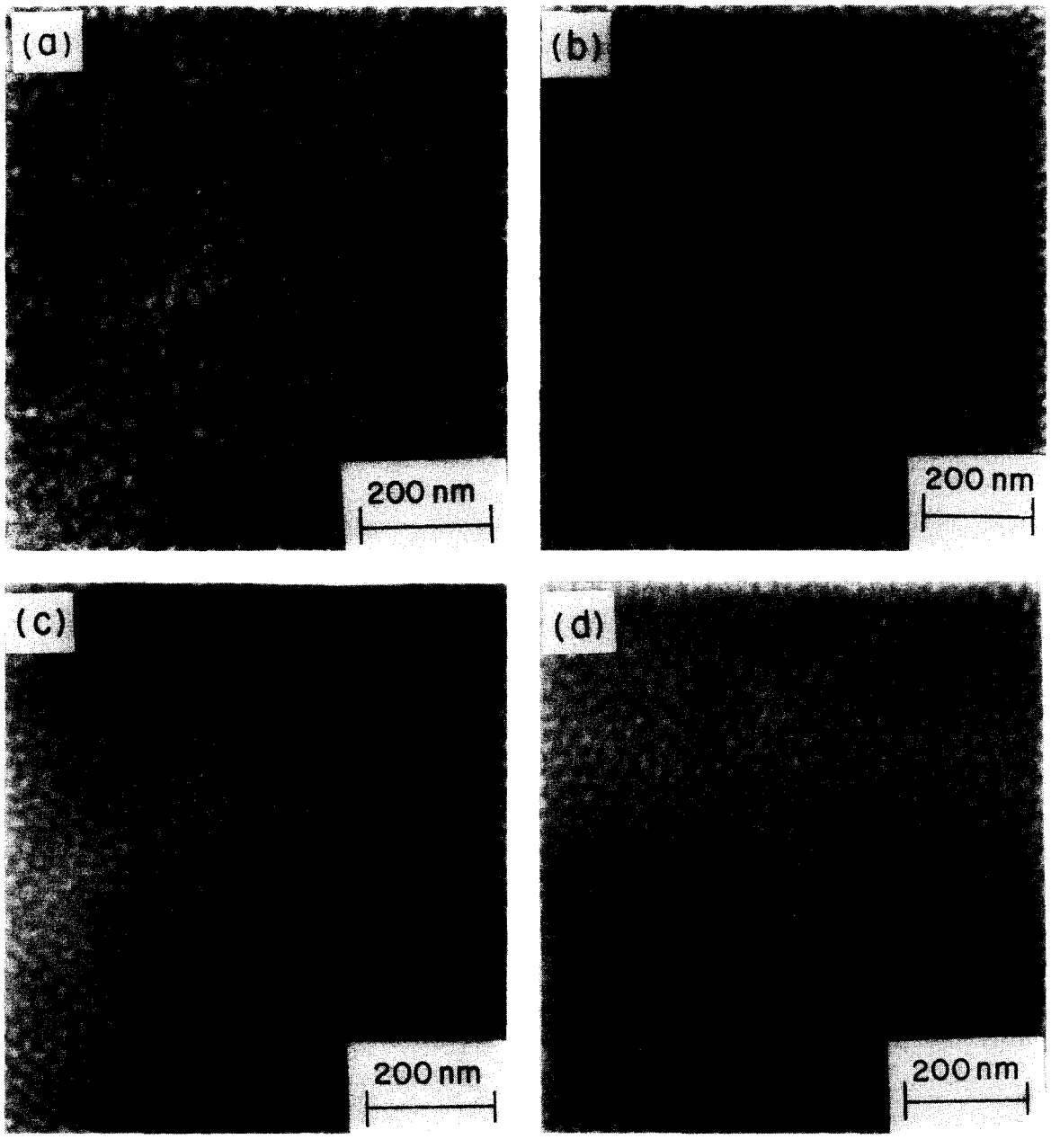

Figure 13 Transmission electron micrographs of ultrathin sections of compression-moulded Kraton 1107 specimens: (a) before being subjected to steady shear flow; (b) cut, after being subjected to steady shear flow at $\dot{\gamma} = 10\ s^{-1}$ in a cone-and-plate rheometer at 200°C, parallel to the shear direction; (c) cut, after being subjected to steady shear flow at $\dot{\gamma} = 100\ s^{-1}$ in a capillary rheometer at 200°C, parallel to the direction of extrusion; (d) cut, after being subjected to steady shear flow at $\dot{\gamma} = 100\ s^{-1}$ in a capillary rheometer at 200°C, perpendicular to the direction of extrusion

at 200°C, perpendicular to the direction of extrusion. In contrast to the situation discussed above for compression-moulded Kraton 1102 specimens, we observe in *Figure 13* that the morphology of compression-moulded Kraton 1107 specimens is affected little by the application of steady shear flow using a cone-and-plate or capillary rheometer. Notice that the shape of PS microdomains (white area) is more or less the same whether the microdomains are viewed along the extrusion direction (see *Figure 13c*) or in the direction perpendicular to the extrusion direction (see *Figure 13d*), suggesting that the PS microdomains are more or less spheres and dispersed in the PI matrix (dark area). It should be mentioned that, previously, Pedemonte and coworkers[25] reported similar observations. Notice in *Figure 13*, however, that the interface between the PS microdomains and the PI matrix in Kraton 1107 is sharper in the sheared specimen than in the unsheared specimen. Note that Kraton 1107 has about 14 wt% PS giving rise to spherical microdomains of the PS phase. We thus speculate that the size (ca. 20 nm) of the spherical microdomains of the PS phase in Kraton 1107 is too small to be deformed noticeably by the application of shear flow employed in the present study. As a matter of fact, this speculation is reflected in the plots of log η *versus* log $\dot{\gamma}$, given in *Figure 2*, showing a gradual decrease in η with increasing $\dot{\gamma}$ from 0.01 to $5\ s^{-1}$. It should be mentioned that the smaller the size of the dispersed phase, the greater would be the shear stress required to deform the suspended droplets in a two-phase system. Owing to the fact that the PS

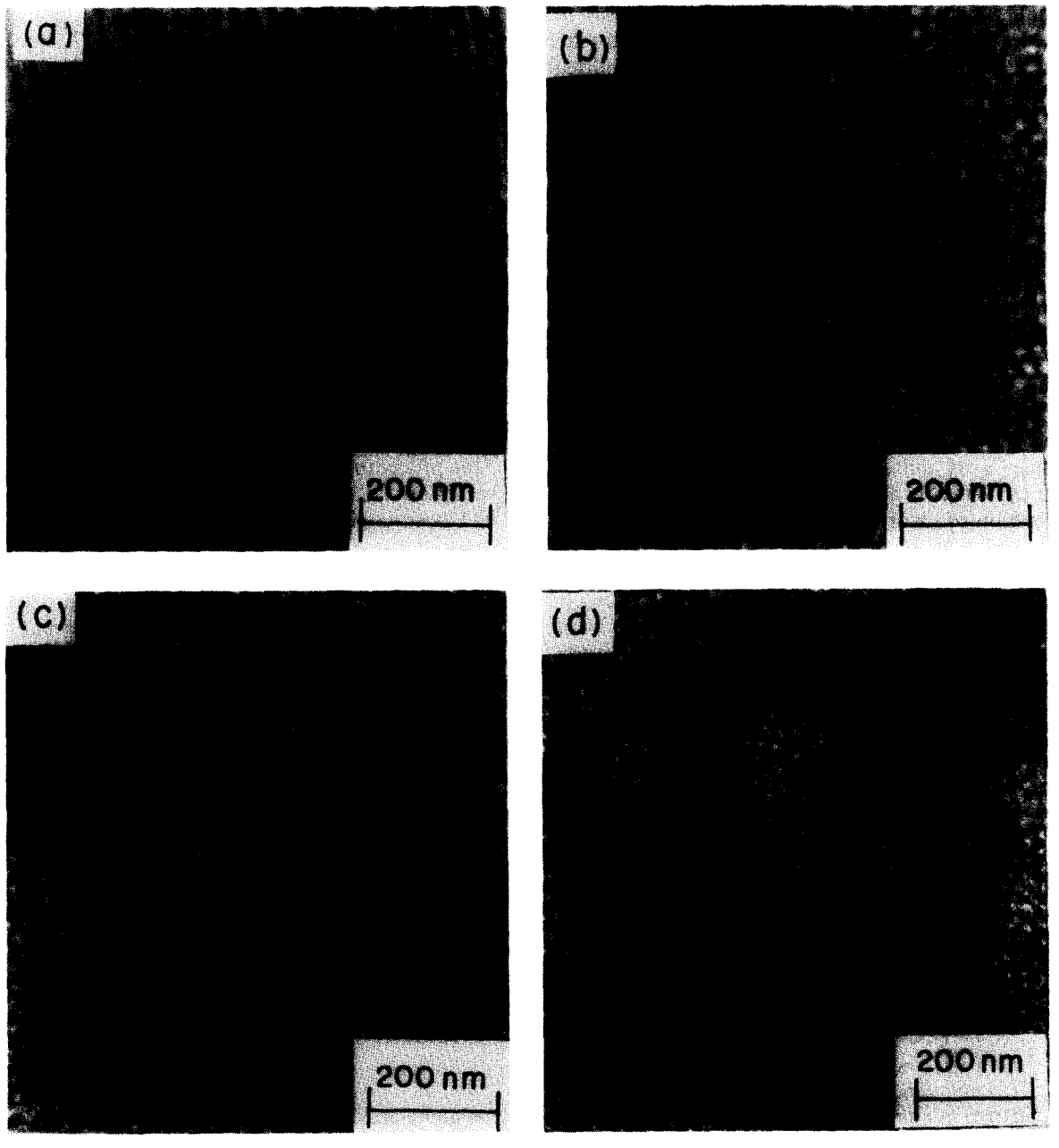

Figure 14 Transmission electron micrographs of ultrathin sections of solvent-cast Kraton 1102 specimens: (a) before being subjected to steady shear flow; (b) cut, after being subjected to steady shear flow at $\dot{\gamma} = 10\ s^{-1}$ in a cone-and-plate rheometer at 200°C, parallel to the direction of shear; (c) cut, after being subjected to steady shear flow at $\dot{\gamma} = 100\ s^{-1}$ in a capillary rheometer at 200°C, parallel to the direction of extrusion; (d) cut, after being subjected to steady shear flow at $\dot{\gamma} = 100\ s^{-1}$ in a capillary rheometer at 200°C, parallel to the direction of extrusion

microdomains in Kraton 1107 are connected to the rubbery PI chains, much greater shear stresses would be required to deform the PS microdomains in Kraton 1107 than droplets freely suspended in a continuous matrix.

Figure 14 gives transmission electron micrographs taken at room temperature of ultrathin sections of solvent-cast Kraton 1102 specimens: (a) before being subjected to steady shear flow; (b) cut, after being sheared at $\dot{\gamma} = 10\ s^{-1}$ in a cone-and-plate rheometer at 200°C, parallel to the direction of shear; (c) cut, after being sheared at $\dot{\gamma} = 100\ s^{-1}$ in a capillary rheometer at 200°C, parallel to the direction of extrusion; and (d) cut, after being sheared at $\dot{\gamma} = 1000\ s^{-1}$ in a capillary rheometer at 200°C, parallel to the direction of extrusion.

The following observations are worth noting in *Figure 14*. (1) In *Figure 14a* we observe that the solvent-cast Kraton 1102 specimen before being subjected to steady shear flow has a morphology exhibiting a regular hexagonal arrangement of PS microdomains (white areas) in the PB matrix (dark areas). Notice that *Figure 14a* for a solvent-cast Kraton 1102 shows much clearer and well defined cylindrical microdomains compared to *Figure 12a* for an as-received sample. (2) Interestingly enough, however, we observe in *Figures 14b–d* that, after being subjected to steady shear flow either in a cone-and-plate rheometer or in a capillary rheometer, the solvent-cast Kraton 1102 has a morphology that is very similar to that of Kraton 1107 (see *Figures 13b* and *13c*). What is rather surprising and unexpected in *Figure 14* is that long rods of PS microdomains were broken

into smaller sizes (which almost look like spheres) at shear rates as low as $10\,s^{-1}$ in the cone-and-plate rheometer. Notice that the diameter of the cylindrical rods of the PS phase is about 5–10 nm (see *Figure 14a*). Notice further in *Figures 14b–d* that the increase of $\dot{\gamma}$ from 10 to $1000\,s^{-1}$ affected little the morphology of the PS phase in the solvent-cast Kraton 1102 specimens. This can easily be understood because the deformation of small spherical domains would have required an enormous stress that was not available during the extrusion in the capillary rheometer. On the basis of the micrographs given in *Figures 14b–d*, we now understand why a gradual decrease in η with increasing $\dot{\gamma}$ was observed when solvent-cast Kraton 1102 specimens were sheared at $0.01–5\,s^{-1}$ in the cone-and-plate rheometer (see *Figure 8*).

It should be mentioned that very recently, using wide-angle X-ray diffraction and transmission electron microscopy, Winey *et al.*[33] and Scott *et al.*[34] showed that an application of shear flow affected the morphology of a block copolymer having lamellar microdomains. The micrographs given in *Figures 12* and *14* for the Kraton 1102 having cylindrical microdomains are in agreement with the experimental observations made by Winey *et al.* and Scott *et al.* We have observed in the present study, however, that an application of shear flow at shear rates as high as $1000\,s^{-1}$ to the Kraton 1107 having spherical microdomains did not affect the morphology of the block copolymer (see *Figure 13*). Owing to the space limitation, micrographs of the Kraton 1107 specimens that were subjected to the shear rate at $1000\,s^{-1}$ are not shown here.

DISCUSSION

Thermal stability of the specimens during rheological measurement

Thermal instability including crosslinking of the block copolymer specimens employed during rheological measurement was of great concern to us, and therefore we investigated the extent of thermal instability, if any, of both Kraton 1102 and Kraton 1107. For this, we determined (a) the gel contents by filtration, and (b) the molecular-weight distribution (i.e. polydispersity index defined by the ratio of weight-average molecular weight to number-average molecular weight) via gel permeation chromatography (g.p.c.).

In determining the gel contents in a polymer sample, we first dissolved the sample in toluene and then filtered the solution using a filter paper having fine pore size (11 μm). Subsequently, the filtrate was dried in a vacuum oven to remove the solvent completely and the weight of the solid phase (i.e. gels) remaining on the filter paper was measured. In conducting the experiments described above, an as-cast or compression-moulded specimen was placed in the cone-and-plate fixture at a predetermined temperature and received thermal treatment for 30 min. This procedure was chosen because we did not save the specimens at the time when rheological measurements had been conducted. In other words, we simulated the thermal history that the specimens experienced during a rheological measurement, which lasted for about 30 min. *Table 1* gives a summary of the gel contents determined for the specimens which had different thermal histories. The following observations are worth noting in *Table 1*. (1) Some gels are present in the virgin (i.e. as-received) polymers. (2) The solvent-cast Kraton 1107 specimen having an antioxidant appears to be thermally very stable even when it was subjected to 220°C for 30 min, whereas the compression-moulded specimen having no antioxidant shows a slightly larger amount of gel when it was subjected to 220°C for 30 min. (3) The solvent-cast Kraton 1102 specimen, when subjected to 180 or 200°C for 30 min, appears to be thermally stable. However, when subjected to 220°C for 30 min, the solvent-cast Kraton 1102 specimen underwent appreciable crosslinking, giving rise to a rapid increase in gel content. (4) The compression-moulded Kraton 1102 specimen, when subjected to 180 or 200°C for 30 min, appears to be

Table 1 Summary of the effect of annealing temperature on the extent of crosslinking and molecular-weight distribution of the block copolymers employed in this study

Polymer	Sample preparation procedure	Thermal history of the specimen	Gel contents (wt%)	Polydispersity index
(a) Virgin polymers				
Kraton 1107[a]	As received	None	1.0	1.19
Kraton 1102[b]	As received	None	0.9	1.15
(b) Thermal treatment				
Kraton 1107	Solvent casting[c]	200°C for 30 min	0.8	1.27
	Solvent casting[c]	220°C for 30 min	1.3	1.51
	Compression moulding	200°C for 30 min	1.3	1.16
	Compression moulding	220°C for 30 min	2.3	1.25
Kraton 1102	Solvent casting[c]	180°C for 30 min	0.5	1.19
	Solvent casting[c]	200°C for 30 min	0.9	1.58
	Solvent casting[c]	220°C for 30 min	32.9	3.70
	Compression moulding	180°C for 30 min	0.7	1.47
	Compression moulding	200°C for 30 min	1.0	1.54
	Compression moulding	220°C for 30 min	16.9	5.48

[a]Kraton 1107 was determined to contain 19.7 wt% diblock copolymer
[b]Kraton 1102 was determined to contain 17.6 wt% diblock copolymer
[c]All solvent-cast samples contained an antioxidant (Irganox 1010, Ciba Geigy Co.) of 0.1 wt%

thermally stable, but the gel contents increase considerably when the specimen was subjected to 220°C for 30 min.

The results of g.p.c. measurements are summarized in the last column of *Table 1*. It should be mentioned that polydispersity index was determined by using the solutions that were collected from the filtration experiment described above. The g.p.c. measurement was conducted to observe variations, if any, in molecular-weight distribution of the specimen after being subjected to a thermal treatment in the rheometer. In *Table 1* we observe a trend that the polydispersity index increases as the gel content in a specimen increases, which can be regarded as being supporting evidence that crosslinking occurred during the thermal treatment at 220°C for 30 min in the cone-and-plate fixture. It should be mentioned that in this paper we do not report any rheological data taken at temperatures higher than 200°C.

Based on the results presented above we conclude that the use of an antioxidant was very effective in minimizing thermal degradation or crosslinking in the Kraton 1102 or Kraton 1107 specimen during the rheological measurement, and that the rheological data presented in *Figures 1, 2, 8, 9, 10* and *11* may be regarded as being reasonably free from thermal degradation or crosslinking of the specimens during rheological measurements. If the extent of gelation were significant, we would expect that (i) the η data taken at 180°C should have been greater than the η data taken at 160 and 170°C for the compression-moulded Kraton 1102 specimens (see *Figure 1*), (ii) the η data taken at 200°C should have been greater than the η data taken at 180°C for the solvent-cast Kraton 1102 specimens (see *Figure 8*), and (iii) the η data taken at 200°C should have been greater than the η data taken at 180°C for the compression-moulded Kraton 1107 specimens (see *Figure 2*). However, we observe in *Figures 1, 2* and *8* that the values of η steadily decrease with increasing temperature, suggesting to us that apparently the extent of gelation was not significant enough to affect the viscosity measurements taken in this study.

Effects of shear history on the viscosity of microphase-separated block copolymers

It should be pointed out, in reference to *Figures 1, 2* and *8*, that the cone-and-plate data at a given temperature were obtained using the same specimen by increasing $\dot{\gamma}$ stepwise, whereas each data point from the capillary rheometer was obtained using a fresh specimen. This means that the cone-and-plate data in *Figures 1, 2* and *8*, except for the data point at the lowest $\dot{\gamma}$, were subjected to shear history (i.e. pre-shearing). Since the block copolymers employed in this study have microdomains and exhibit yield behaviour, we thought that it is reasonable to expect that pre-shearing a specimen might influence the subsequent rheological behaviour. This expectation is based on the recent experimental observation by Kim and Han[35], who reported the effect of shear history on the steady shear flow properties of a thermotropic liquid-crystalline polymer (TLCP), which also exhibited yield behaviour and had domain textures at the nematic state.

In order to investigate the effect, if any, of shear history on the subsequent rheological behaviour of the block copolymers employed in this study, we compared both transient and steady-state shear flow behaviour of fresh

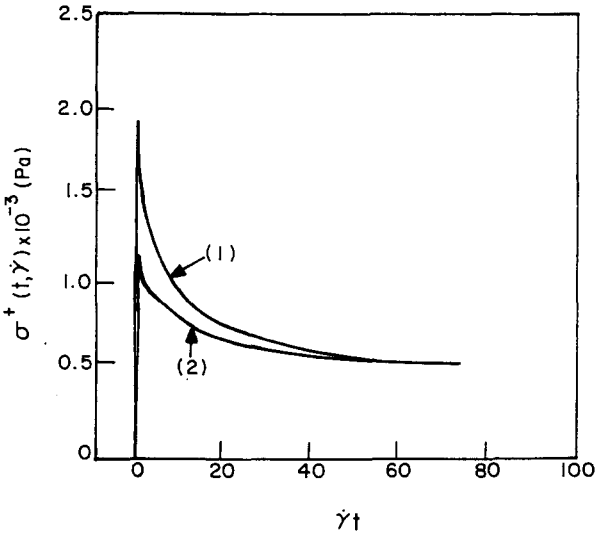

Figure 15 Traces of $\sigma^+(t,\dot{\gamma})$ *versus* $\dot{\gamma}t$ for solvent-cast Kraton 1102 specimens at 180°C at $\dot{\gamma}=0.1\ s^{-1}$: curve 1 for a fresh specimen and curve 2 for a specimen pre-sheared at $\dot{\gamma}=0.01\ s^{-1}$ for 10 min

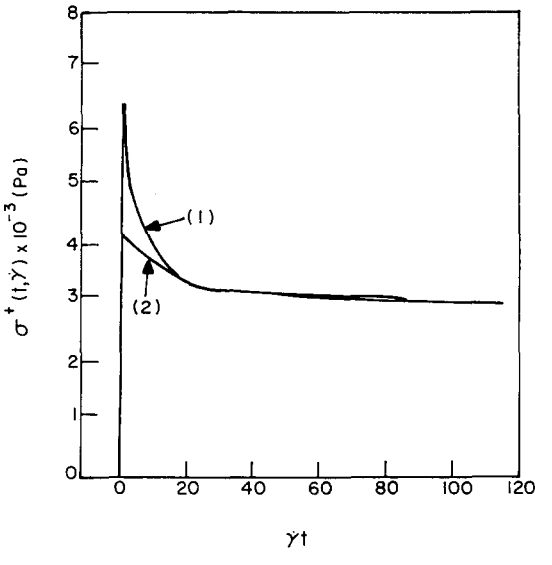

Figure 16 Traces of $\sigma^+(t,\dot{\gamma})$ *versus* $\dot{\gamma}t$ for solvent-cast Kraton 1102 specimens at 180°C at $\dot{\gamma}=1.0\ s^{-1}$: curve 1 for a fresh specimen and curve 2 for a specimen pre-sheared at $\dot{\gamma}=0.1\ s^{-1}$ for 5 min

and pre-sheared specimens under otherwise identical conditions. Plots of $\sigma^+(t,\dot{\gamma})$ *versus* $\dot{\gamma}t$ for solvent-cast Kraton 1102 specimens at 180°C are given in *Figure 15*, where curve 1 represents the rheological response at $\dot{\gamma}=0.1\ s^{-1}$ of a fresh specimen and curve 2 represents the rheological response at $\dot{\gamma}=0.1\ s^{-1}$ of a specimen that had been pre-sheared at $\dot{\gamma}=0.01\ s^{-1}$ for 10 min. It is of interest to observe in *Figure 15* that the magnitude of the stress overshoot is much larger in the fresh specimen than that in the pre-sheared specimen, but the steady-state value of shear stress is affected little by pre-shearing at $\dot{\gamma}=0.01\ s^{-1}$. Similar observation can be made in *Figure 16*, where curve 1 represents the rheological response at $\dot{\gamma}=1\ s^{-1}$ of a fresh specimen and curve 2 represents the rheological response at $\dot{\gamma}=1\ s^{-1}$ of a specimen that had been pre-sheared at $\dot{\gamma}=0.1\ s^{-1}$ for 5 min. It is of interest to observe that in *Figure 15* the ratio of the shear stress

overshoot to the steady-state shear stress, σ_{max}/σ_s, is about 3 for the fresh specimen and about 2 for the pre-sheared specimen, and that in *Figure 16* the ratio σ_{max}/σ_s is about 1.9 for the fresh specimen and about 1.2 for the pre-sheared specimen.

In their paper, Kim and Han[36] noted that the very large values of σ_{max}/σ_s (ca. 8–12) were observed for a TLCP and it was attributed to a break-up of the polydomain texture that existed in the specimen before being subjected to a sudden shear flow. We believe that the relatively large values of σ_{max}/σ_s observed in *Figures 15* and *16* for the block copolymer Kraton 1102, although much smaller than those for the TLCP reported by Kim and Han[36], are attributable to the disruption, upon start-up of shear flow, of the cylindrical microdomains that existed in the specimen before being subjected to a sudden shear flow. It should be remembered that in *Figure 14* we presented experimental evidence that indeed the morphology of the solvent-cast Kraton 1102 specimen changed after being subjected to a shear flow at $\dot{\gamma} = 10\ s^{-1}$ in the cone-and-plate rheometer and at higher values of $\dot{\gamma}$ in the capillary rheometer.

Considering the facts that the sizes of the microdomains in Kraton 1102 are very small (say, less than 50 nm diameter) compared to the sizes of the domain texture (ca. 1–10 μm) in a typical TLCP and that the cylindrical microdomains in Kraton 1102 are chemically joined to the mid-block polybutadiene chains, we can anticipate that the extent of disruption, upon start-up of shear flow, of the morphology that existed in the block copolymer specimen before being subjected to shear flow would be much less than the extent of break-up of polydomain textures in a TLCP. This probably might be the reason why the value of σ_{max}/σ_s for the block copolymer, Kraton 1102, observed in *Figures 15* and *16* is much smaller than that for TLCP.

Failure of time–temperature superposition for microphase-separated block copolymers

In the past, a number of investigators[10,13,18] have used time–temperature superposition to obtain reduced (or master) curves from either oscillatory shear flow data or steady shear flow data for microphase-separated block copolymers. However, it can be clearly seen from *Figures 1*, *2* and *8* that one cannot obtain a temperature-independent master curve by shifting the viscosity curves obtained at other temperatures to a viscosity curve obtained at a particular temperature (as a reference temperature), i.e. time–temperature superposition fails for the block copolymers, Kraton 1102 and Kraton 1107, in the temperature range investigated. Earlier, Tschoegl and coworkers[37–40] pointed out that time–temperature superposition fails for microphase-separated block copolymers.

According to a previous study by Han *et al.*[20], Kraton 1102 has cylindrical microdomains at temperatures below ca. 220°C and Kraton 1107 has spherical microdomains at temperatures below ca. 230°C. Han and coworkers[19–21] claimed that time–temperature superposition fails as long as the segmental miscibility in a given block copolymer (i.e. solubilization of microdomains in the matrix phase) varies with increasing or decreasing temperature. In other words, as the temperature increases towards the order–disorder transition temperature at which a block copolymer becomes completely homogeneous (or isotropic), the solubilization of the microphase-separated component into the matrix phase increases, thus leaving lesser amounts of microphase-separated component remaining. Thus, from a rheological point of view, a microphase-separated block copolymer can be regarded as being a different material at each temperature and therefore time–temperature superposition is expected to fail for such polymers.

CONCLUDING REMARKS

In this paper we have presented experimental results showing that the morphology of a block copolymer influences greatly its rheological behaviour, with emphasis on the effects of the method of sample preparation and flow geometry employed. Specifically, we have presented steady shear viscosities for compression-moulded and solvent-cast SBS triblock copolymers (Kraton 1102), as well as a compression-moulded SIS triblock copolymer (Kraton 1107), which were measured using both cone-and-plate and capillary rheometers. Transmission electron microscopy was used to investigate the morphology of the specimens before and after being subjected to steady shear flow.

From the present study we have made the following observations. (1) The steady shear viscosities obtained using a cone-and-plate rheometer did not overlap those obtained using a capillary rheometer for compression-moulded block copolymer specimens, while a reasonably good agreement was obtained between the two for solvent-cast block copolymer specimens. (2) The shear-thinning behaviour at low shear rates ($0.01 < \dot{\gamma} < 5\ s^{-1}$) is much stronger in compression-moulded Kraton 1102 specimens than in compression-moulded Kraton 1107 specimens (compare *Figure 1* with *Figure 2*). This is attributable to the fact that the morphology of the compression-moulded Kraton 1102 specimen was affected greatly by shear flow (see *Figure 12*), whereas the morphology of compression-moulded Kraton 1107 was affected little by shear flow (see *Figure 13*). (3) Over a wide range of $\dot{\gamma}$ tested the solvent-cast Kraton 1102 specimens give rise to much lower values of η, as compared to the compression-moulded specimens. This is attributable to the differences in the morphology that existed in the respective specimens. (4) Time–temperature superposition is not applicable to microphase-separated block copolymers. (5) The application of steady shear flow affected little the morphology of the compression-moulded Kraton 1107 specimen having spherical microdomains. (6) The complex shear viscosities do not overlap the steady shear viscosities at the same shear rates and angular frequencies, indicating that the Cox–Merz rule does not hold for microphase-separated block copolymers.

ACKNOWLEDGEMENTS

We would like to thank Mrs T. T. Young for her assistance in obtaining the transmission electron micrographs reported in this paper. We are very grateful for the very constructive comments made by an anonymous referee, which helped us to improve the content of our original manuscript.

REFERENCES

1 Han, C. D. 'Multiphase Flow in Polymer Processing', Academic Press, New York, 1981
2 Han, C. D. and Yu, T. C. *J. Appl. Polym. Sci.* 1971, **15**, 1163
3 Han, C. D. *J. Appl. Polym. Sci.* 1971, **15**, 2579
4 Han, C. D. and Yu, T. C. *Polym. Eng. Sci.* 1972, **12**, 81
5 Han, C. D. and Kim, Y. W. *Trans. Soc. Rheol.* 1975, **19**, 245
6 Han, C. D. and Kim, Y. W. *J. Appl. Polym. Sci.* 1975, **19**, 2831
7 Kim, Y. W. and Han, C. D. *J. Appl. Polym. Sci.* 1976, **20**, 2905
8 Kraus, G. and Gruver, J. T. *J. Appl. Polym. Sci.* 1967, **11**, 2121
9 Holden, G., Bishop, E. T. and Legge, N. R. *J. Polym. Sci. (C)* 1969, **26**, 37
10 Chung, C. I. and Gale, J. C. *J. Polym. Sci., Polym. Phys. Edn.* 1976, **14**, 1149
11 Vinogradov, G. V., Dreval, V. E., Malkin, A. Ya., Yanovsky, Yu. G., Barancheeva, V. V., Borisenkova, E. K., Zabugina, M. P., Plotnikova, E. P. and Sabsai, O. Yu. *Rheol. Acta* 1978, **17**, 258
12 Ghijsels, A. and Raadsen, J. *Pure Appl. Chem.* 1980, **52**, 1359
13 Arnold, K. R. and Meier, D. J. *J. Appl. Polym. Sci.* 1970, **14**, 427
14 Chung, C. I. and Lin, M. I. *J. Polym. Sci., Polym. Phys. Edn.* 1978, **16**, 545
15 Futamura, S. and Meinecke, E. A. *Polym. Eng. Sci.* 1977, **17**, 563
16 Guinlock, E. and Porter, R. S. *Polym. Eng. Sci.* 1977, **17**, 535
17 Widmaier, J. M. and Meyer, C. C. *J. Polym. Sci. (B) Polym. Phys.* 1980, **18**, 2217
18 Bates, F. S. *Macromolecules* 1984, **17**, 2607
19 Han, C. D. and Kim, J. *J. Polym. Sci. (B) Polym. Phys.* 1987, **25**, 1741
20 Han, C. D., Kim, J. and Kim, J. K. *Macromolecules* 1989, **22**, 383
21 Han, C. D., Baek, D. M. and Kim, J. *Macromolecules* 1990, **23**, 561
22 Han, C. D., Baek, D. M., Kim, J. K. and Chu, S. G. *Polymer* 1992, **33**, 294
23 Meier, D. *J. Polym. Sci. (C)* 1969, **26**, 81
24 Uchida, T., Soen, T., Inoue, T. and Kawai, H. *J. Polym. Sci. (A-2)* 1972, **10**, 101
25 Pedemonte, E., Turturro, A., Bianchi, U. and Devetta, P. *Polymer* 1973, **14**, 145
26 Thomas, E. L., Alward, D. B., Kinning, D. J., Martin, D. C., Hardlin, D. L. and Fetters, L. J. *Macromolecules* 1986, **19**, 2197
27 Hasegawa, H., Tanaka, H., Yamasaki, K. and Hashimoto, T. *Macromolecules* 1987, **20**, 1651
28 Inoue, T., Soen, T., Hashimoto, T. and Kawai, H. *J. Polym. Sci. (A-2)* 1969, **7**, 1283
29 Cox, W. P. and Merz, E. H. *J. Polym. Sci.* 1958, **28**, 619
30 Keller, A., Pedemonte, E. and Willmouth, F. M. *Nature* 1970, **225**, 538
31 Keller, A., Pedemonte, E. and Willmouth, F. M. *Kolloid Z. Z. Polym.* 1970, **238**, 385
32 Pedemonte, E., Dondero, G., Alfonso, G. C. and de Candia, F. *Polymer* 1975, **16**, 531
33 Winey, K. I., Patel, S. S., Larson, R. G. and Watanabe, H. *Macromolecules* 1993, **26**, 2542
34 Scott, D. B., Waddon, A. J., Lin, Y. G., Karasz, F. E. and Winter, H. H. *Macromolecules* 1992, **25**, 4175
35 Kim, S. S. and Han, C. D. *J. Polym. Sci., Polym. Phys. Edn.* 1994, **32**, 371
36 Kim, S. S. and Han, C. D. *J. Rheol.* 1993, **37**, 847; 1994, **38**, 31
37 Lim, C. K., Cohen, R. E. and Tschoegl, N. W. in 'Multicomponent Polymer Systems', *Adv. Chem. Ser.* **99** (Ed. N. A. J. Platzer), American Chemical Society, Washington, DC, 1971, p. 397
38 Fesko, D. G. and Tschoegl, N. W. *J. Polym. Sci. (C)* 1971, **35**, 51
39 Fesko, D. G. and Tschoegl, N. W. *Int. J. Polym. Mater.* 1974, **3**, 51
40 Cohen, R. E. and Tschoegl, N. W. *Trans. Soc. Rheol.* 1976, **20**, 153